# Structural evolution and stabilities of neutral and anionic clusters of lead sulfide: Joint anion photoelectron and computational studies

Pratik Koirala,[1] Boggavarapu Kiran,[2] Anil K. Kandalam,[1,a)] Charles. A. Fancher,[3] Helen L. de Clercq,[3] Xiang Li,[3] and Kit. H. Bowen[3,a)]

[1]*Department of Physics, McNeese State University, Lake Charles, Louisiana 70609, USA*
[2]*Department of Chemistry, McNeese State University, Lake Charles, Louisiana 70609, USA*
[3]*Department of Chemistry and Material Sciences, Johns Hopkins University, Baltimore, Maryland 21218, USA*

The geometric and electronic structures of both neutral and negatively charged lead sulfide clusters, $(PbS)_n/(PbS)_n^-$ ($n = 2$–10) were investigated in a combined anion photoelectron spectroscopy and computational study. Photoelectron spectra provided vertical detachment energies (VDEs) for the cluster anions and estimates of electron affinities (EA) for their neutral cluster counterparts, revealing a pattern of alternating EA and VDE values in which even $n$ clusters exhibited lower EA and VDE values than odd $n$ clusters up until $n = 8$. Computations found neutral lead sulfide clusters with even $n$ to be thermodynamically more stable than their immediate (odd $n$) neighbors, with a consistent pattern also being found in their HOMO–LUMO gaps. Analysis of neutral cluster dissociation energies found the $Pb_4S_4$ cube to be the preferred product of the queried fragmentation processes, consistent with our finding that the lead sulfide tetramer exhibits enhanced stability; it is a magic number species. Beyond $n = 10$, computational studies showed that neutral $(PbS)_n$ clusters in the size range, $n = 11$–15, prefer two-dimensional stacking of face-sharing lead sulfide cubical units, where lead and sulfur atoms possess a maximum of five-fold coordination. The preference for six-fold coordination, which is observed in the bulk, was not observed at these cluster sizes. Taken together, the results show a preference for the formation of slightly distorted, fused cuboids among small lead sulfide clusters. © 2011 American Institute of Physics. [doi:10.1063/1.3635406]

## I. INTRODUCTION

Semiconductor nanocrystals or quantum dots (QDs) have attracted considerable interest in recent years due to their size-tunable electronic and optical properties. By virtue of the spatial confinement of excitons (electron-hole pairs), QDs have applications in diverse fields such as optoelectronics and bio-medicine. Substantial progress has been made in recent years, in the preparation, characterization, and fundamental study of QDs. Numerous methods have been devised to synthesize colloidal QDs in various sizes and shapes often in diverse environments, e.g., in solutions, embedded in zeolites, in glasses, and in semiconducting polymers. Although the vast majority of QD research is focused on Group II-VI and III-V systems, narrow bandgap semiconductor materials, such as lead sulfide (0.286 eV at 4.2 K and 0.41 eV at room temperature)[1,2] have unique advantages. Unlike other semiconducting quantum dots, such as CdSe, lead sulfide has a large exciton Bohr radius (18 nm for PbS versus 5.3 nm for CdSe), allowing it to exhibit strong quantum confinement effects at much larger sizes than in CdSe.

Despite the importance of lead sulfide in the ultra-small size regime, experimental investigations of lead sulfide molecules and clusters have been limited. Work which has been reported includes mass spectrometric studies of $(PbS)^+_{1-4}$ cluster cations,[3,4] spectroscopic investigations of neutral lead sulfide monomers and dimers in both matrices and the gas phase,[5,6] and a lone photoelectron spectroscopic study of the $(PbS)^-$ molecular anion.[7] Molecular size, uncapped PbS quantum dots,[8] as well as colloidal PbS quantum dots[9] have also been the focus of experimental studies.

While lead sulfide nanocrystals, quantum dots, and nanorods have been the focus of many computational studies,[10–12] relatively few calculations have been conducted on lead sulfide clusters. Those calculations include two DFT studies which investigated the stability and optical properties of neutral $(PbS)_n$ clusters.[13,14] To our knowledge, neither experimental nor theoretical studies of negatively charged lead sulfide clusters exist in literature. In order to gain a better understanding of the structural evolution and electronic structure of small lead sulfide clusters, we conducted a synergetic experimental and computational study of their anions and corresponding neutrals, $(PbS)_n^-$ and $(PbS)_n$, respectively. Here, we present the results of our joint anion photoelectron spectroscopic (PES) and density functional theory (DFT) study of $(PbS)_n^-$ and $(PbS)_n$ clusters, $n = 2$–10. In addition, we also report DFT-based computational results on the structural evolution and the stability of slightly larger $(PbS)_n$ neutral clusters over the size range, $n = 11$–15.

a)Authors to whom correspondence should be addressed. Electronic addresses: akandalam@mcneese.edu and kbowen@jhu.edu.

## II. METHODOLOGIES

### A. Experimental method

Lead sulfide cluster anions were generated in a "smoke-ion" source which has been described in detail previously.[15] This device consists of an inert gas condensation cell coupled to a weakly ionized plasma for the formation of ions of high temperature materials. In this experiment, lead sulfide powder (99.5% ESPI) was evaporated from a quartz crucible heated with a tungsten heating coil to a temperature of 800 K. The vapor was then rapidly cooled in a 2.0 Torr helium environment, held at 273 K, and ionized with a filament biased between $-50$ and $-100$ V (10 mA electron emission current). This resulted in a mass spectrum of lead sulfide nanocluster anions ranging in size from 14–56 PbS molecules per cluster. When the filament bias was increased to between $-150$ and $-200$ V, a discontinuous mass spectrum was produced containing a second, smaller size distribution of anionic molecules and clusters, comprising 1 to 12 PbS molecules per cluster as well as the larger size distribution already mentioned. Cluster anions in this smaller size distribution were then probed with negative ion PES.

Anion photoelectron spectroscopy is conducted by crossing a mass-selected beam of negative ions with a fixed-frequency photon beam and energy analyzing the resultant photodetached electrons.[16] This technique is a direct approach to measuring electron binding energies, and it is governed by the energy-conserving relationship, $h\nu = \text{EBE} + \text{EKE}$, where $h\nu$ is the photon energy, EBE is the electron binding (transition) energy, and EKE is the measured electron kinetic energy. Our apparatus consists of the "smoke-ion" source, ion optics, a magnetic sector mass analyzer/sector, an argon ion laser operated intra-cavity, and a hemispherical electron analyzer (resolution of 23 meV). The photoelectron spectra of $(\text{PbS})_n^-$ were recorded using both the 488.0 nm (2.540 eV) and 457.9 nm (2.707 eV) lines of an argon ion laser, and they were calibrated against the well-known photoelectron spectrum of $O^-$. There was no apparent EBE difference in the recorded photoelectron spectra upon switching between these two photon energies.

### B. Computational method

Calculations were carried out under the framework of density functional theory using GAUSSIAN03 software.[17] We used the gradient-corrected PW91PW91 functional,[18] while the compact effective potentials (CEPs) due to Stevens *et al.*[19] (SBKJC) and $6-311+G^*$ basis sets were used for lead and sulfur atoms, respectively. In the two previously reported DFT-based studies on $(\text{PbS})_n$ clusters,[13,14] the hybrid DFT functional, Becke's three parameter hybrid exchange functional with Lee, Yang, and Parr correlation functional (B3LYP),[20,21] was employed. In order to verify the accuracy of our density functional as well as the basis set (SBKJC) for the lead atoms, we calculated the adiabatic detachment energy (ADE) and vertical detachment energy (VDE) of the $\text{Pb}_6\text{S}_6^-$ cluster using both B3LYP and PW91PW91 functionals, along with two different basis sets for Pb, namely, the Stuttgart/Dresden (SDD) basis set[22] and SBKJC. These val-

TABLE I. Comparison of various functional forms and different basis functions on $(\text{PbS})_6^-$. The relative energy ($\Delta E$), VDE, and ADE (in eV) for two isomers (6a′ and 6b′) along with the experimental values are also given.

| | $(\text{PbS})_6^-$ | | | | | |
| | Cage (6b′) | | | Double-cube (6a′) | | |
| Functional/basis | $\Delta E$ | VDE | ADE | $\Delta E$ | VDE | ADE |
|---|---|---|---|---|---|---|
| B3LYP/SDD | 0.00 | 3.09 | 2.08 | 0.39 | 1.50 | 1.46 |
| B3LYP/SBKJC | 0.00 | 3.15 | 2.08 | 0.02 | 1.75 | 1.61 |
| PW91/SDD | 0.00 | 3.01 | 2.61 | 0.30 | 1.70 | 1.67 |
| PW91/SBKJC | 0.27 | 3.14 | 2.38 | 0.00 | 2.00 | 1.79 |
| Experiment | 2.00 (VDE); 1.74 (ADE) | | | | | |

ues were then compared with our corresponding experimental values. The results from these benchmark calculations are given in Table I. Two isomers, a cage structure and an isomer with face-sharing cubes, were considered for $\text{Pb}_6\text{S}_6^-$ cluster. Our calculations indicated that the PW91PW91 functional along with the SBKJC basis set for lead atoms results in a better agreement with the experimental VDE and ADE, while a strong disagreement is observed for SDD basis set, irrespective of the functional form. Thus, in what follows, we will report results based only on the PW91PW91 functional form with the SBKJC basis set. In the procedure for geometry optimization, the convergence in total energy and gradient was set to $10^{-9}$ hartree and $10^{-4}$ hartree/Å, respectively. The stability of all the isomers considered in this study was verified by carrying out vibrational frequency calculations.

Vertical detachment energies were calculated as the energy differences between the neutral and anionic clusters, calculated at the anions' ground state geometry. The adiabatic detachment energy was obtained by calculating the energy difference between the ground state geometry (its lowest energy isomer) of the anionic cluster and the structurally similar isomer of its neutral counterpart. Since several nearly isoenergetic isomers ($\Delta E \sim 0.20$ eV) were found for some cluster sizes, their presence or absence in the molecular beam were assessed by comparing their calculated ADE and VDE values with the corresponding values obtained from their photoelectron spectra.

## III. RESULTS AND DISCUSSION

### A. Experimental results and discussion

The photoelectron spectra of $(\text{PbS})_n^-$, $n = 1$–10 are presented in Fig. 1. The bottom x-axis shows the electron kinetic energy (EKE) scale, while the top x-axis displays the electron binding energy (EBE) scale, these being related by the relation, $\text{EKE} = h\nu - \text{EBE}$. Most of these spectra are dominated by single, strong peaks, the exception being the spectrum of the dimer anion. In the dimer anion's case, the higher EBE peak is due to a transition between the anion's ground state and the first excited state of the corresponding neutral. Additionally, the spectrum of $(\text{PbS})_8^-$ exhibits a low intensity feature at EBE $\sim$1.7 eV on the low EBE side of its main peak, and a similar feature is seen as a shoulder in the spectrum of $(\text{PbS})_5^-$. The weak features in the spectra of $(\text{PbS})_8^-$
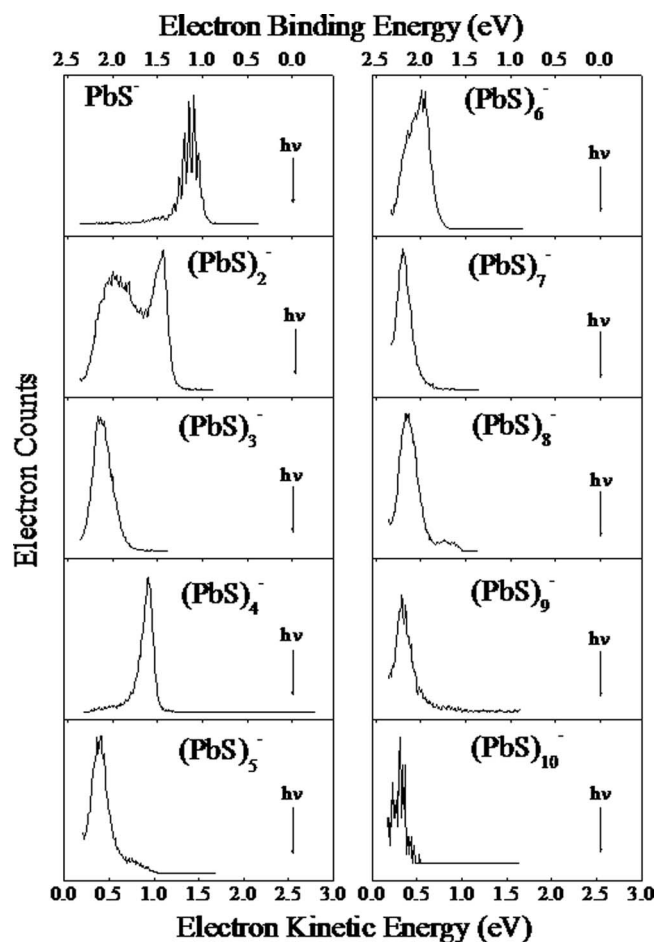
## Electron Binding Energy (eV)



FIG. 1.  The 488 nm photoelectron spectra of the stoichiometric lead sulfide cluster anion series, $(PbS)_n^-$ ($n = 1–10$).

TABLE II. The measured and calculated adiabatic detachment energy and vertical detachment energy of $(PbS)_n^-$ ($n = 1–10$) clusters.

| Cluster | Structure | Experimental value (eV) | | Theoretical value (eV) | |
|---|---|---|---|---|---|
| | | ADE | VDE | ADE | VDE |
| $PbS^-$ | 1a′ | 1.05 | 1.10 | 0.91 | 1.00 |
| $(PbS)_2^-$ | 2a′ | 1.30 | 1.50 | 1.62 | 1.70 |
| $(PbS)_3^-$ | 3a′ | 1.89 | 2.20 | 2.00 | 2.19 |
| | 3b′ | | | 2.72 | 2.31 |
| $(PbS)_4^-$ | 4a′ | 1.47 | 1.66 | 1.44 | 1.81 |
| $(PbS)_5^-$ | 5a′ | 1.95 | 2.10 | 1.74 | 1.95 |
| | 5b′ | | | 2.23 | 3.07 |
| $(PbS)_6^-$ | 6a′ | 1.74 | 2.00 | 1.79 | 2.00 |
| | 6b′ | | | 2.38 | 3.14 |
| | 6c′ | | | 1.66 | 1.79 |
| $(PbS)_7^-$ | 7a′ | 2.01 | 2.22 | 2.17 | 2.32 |
| | 7b′ | | | 1.86 | 2.41 |
| $(PbS)_8^-$ | 8a′ | 1.93 | 2.25 | 1.89 | 2.35 |
| | 8b′ | | | 1.90 | 2.11 |
| $(PbS)_9^-$ | 9a′ | 1.99 | 2.15 | 1.99 | 2.04 |
| | 9b′ | | | 1.85 | 2.02 |
| $(PbS)_{10}^-$ | 10a′ | 2.08 | 2.25 | 2.12 | 2.32 |
| | 10b′ | | | 2.14 | 2.36 |
| | 10c′ | | | 2.06 | 2.32 |

and $(PbS)_5^-$ may be due to vibrational hot bands, but they are more likely due to the higher energy isomers. The lowest EBE peak in the dimer anion and the main peaks in all of the other spectra correspond to transitions between their cluster anion electronic ground states and the lowest energy, accessible electronic states of their corresponding neutral clusters.

The widths of the spectra also deserve comment. The lower EBE feature in the dimer anion's spectrum exhibits a width, which is similar to that seen for the main peaks of the larger cluster anions. In fact, the widths of all of these are remarkably similar and, given their complexity, relatively narrow. This suggests that the neutral state being accessed in these transitions is structurally similar to that of the cluster anion, vindicating the use of the computational definition of ADE described above. Also, as shown below, the calculated anion/neutral structures of these species often show close geometric similarities.

Vertical detachment energies were taken to be the EBE values of the intensity maxima in the main peaks and the lowest EBE peak in the case of the dimer anion. Adiabatic detachment energies were taken as the EBE values at ~10% of the peak heights of Gaussian fits of the main peaks (or the low EBE peak in the case of $n = 2$) on their low EBE sides. The measured ADE and VDE values along with the computed ADE and VDE are listed in Table II. (Note: Our computations

agree that the VDE value for $(PbS)_8^-$ is appropriately associated with its main peak.)

Both Fig. 1 and Table II reveal an odd-even alteration of VDE and ADE values in which even $n$ clusters exhibit lower ADE and VDE values than odd $n$ clusters at least up to $n = 8$. This alteration bears a resemblance to the photoelectron spectra of sodium fluoride cluster anions,[23] contrasting with that of covalently bonded, gallium arsenide cluster anions, which show no such alternation.[24] This is consistent with lead sulfide clusters showing a marked tendency toward ionic behavior, i.e., fused cuboid and "baby crystal" formation. Finally, lead sulfide tetramers, $(PbS)_4/(PbS)_4^-$, exhibit remarkably low ADE and VDE values relative to their immediate size neighbors, i.e., $n = 3$ and 5. Our computational results, presented below, demonstrate the uniqueness of lead sulfide tetramer, cuboids among $(PbS)_n$ ($n = 1–10$) clusters.

### B. Theoretical results and discussion

Figures 2 and 3 display the ground state geometries and higher energy isomers of neutral and anionic $(PbS)_n/(PbS)_n^-$ ($n = 1–10$) clusters. The calculated and measured adiabatic detachment energies and vertical detachment energies are given in Table II.

#### 1. Neutral and negatively charged $(PbS)_n$ ($n = 1–10$) clusters

*a. PbS/PbS⁻.*    The bond length of PbS is calculated to be 2.30 Å, while in its anionic counterpart the bond length has elongated to 2.40 Å. Using the Franck-Condon analysis of the photoelectron spectrum of $PbS^-$, one of the current authors (K.H.B.) earlier reported[7] the bond length of $PbS^-$ to be
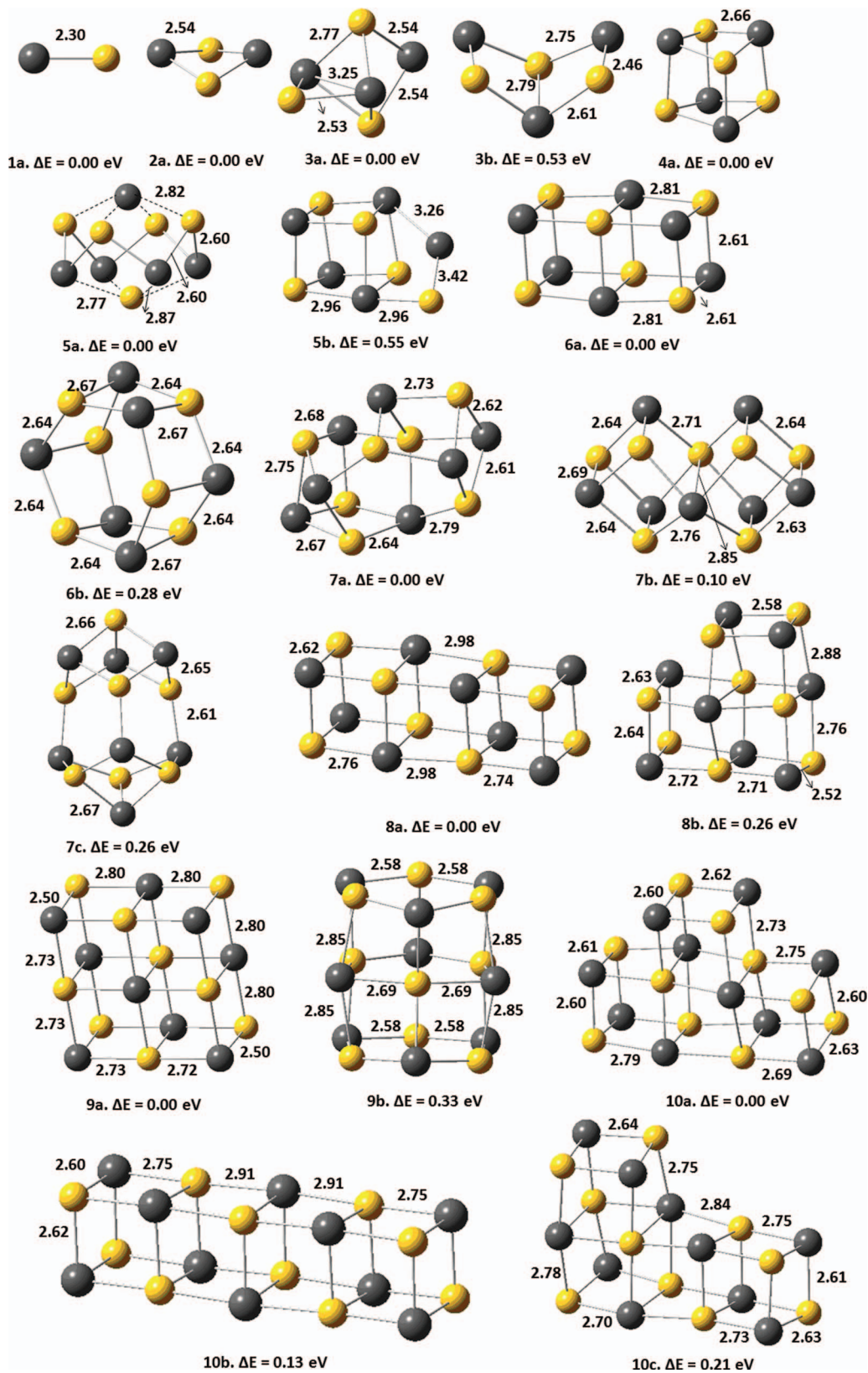
FIG. 2. The lowest energy and higher energy isomers of neutral $(PbS)_n$ ($n = 1$–10) clusters. The yellow spheres represent S atoms and the grey ones represent Pb atoms. The bond lengths are given in Å. The relative energy is calculated with respect to the lowest energy structure.
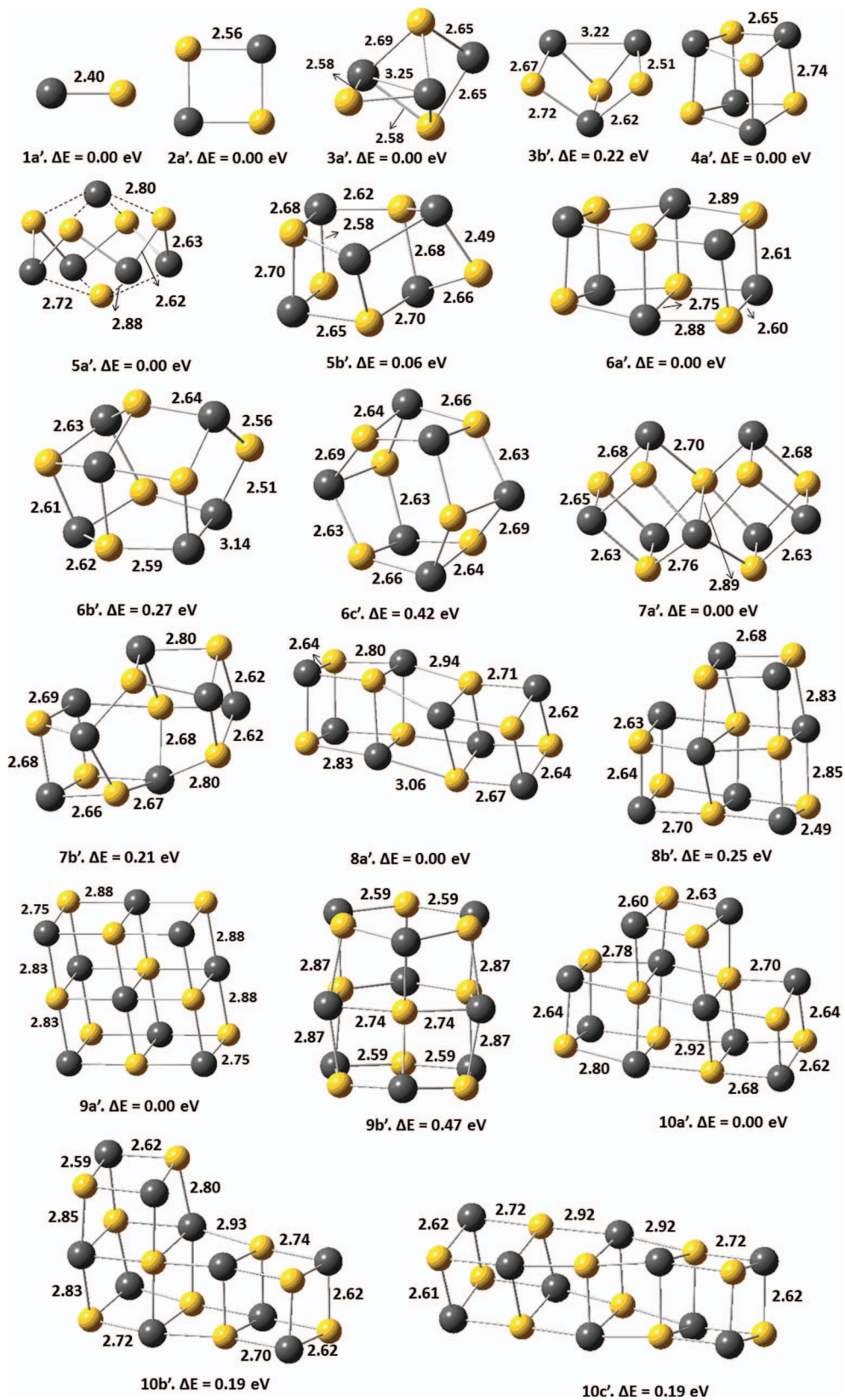
FIG. 3.  The lowest energy and higher energy isomers of anionic $(PbS)_n$ ($n = 1–10$) clusters. The yellow spheres represent S atoms and the grey ones represent Pb atoms. The bond lengths are given in Å. The relative energy is calculated with respect to the lowest energy structure.

2.39 Å. The VDE and ADE of $PbS^-$/PbS were calculated to be 1.0 eV and 0.91 eV, respectively, while the corresponding measured values are 1.10 and 1.05 eV, respectively. Thus, our calculated bond length and the electron detachment energies are in excellent agreement with the experimental values.

*b. $(PbS)_2$/$(PbS)_2^-$.* In the case of $(PbS)_2$ and $(PbS)_2^-$, two structures were considered for geometry optimization, with one being a square and the other a non-planar bent structure. In both structures, the Pb and S atoms are arranged in an alternate fashion. The square structure (Fig. 3, 2a′) is found to be the ground state for the $(PbS)_2^-$, while the neutral $(PbS)_2$ prefers the bent structure (Fig. 2, 2a), with a folding angle of 16.86°. Interestingly, the square structure is not even a minimum in neutral $(PbS)_2$, while the bent structure is not a minimum on the potential energy surface of $(PbS)_2^-$. The separation between the Pb atoms in $(PbS)_2^-$ is 3.59 Å, while neutral $(PbS)_2$ exhibits an increased interaction between Pb atoms resulting in the bent structure with Pb atoms separated by 3.39 Å. On the other hand, the Pb–S bond lengths are almost equal in both the neutral and anionic dimers, with 2.54 Å in neutral and 2.56 Å in anion. These bond lengths are longer than in their corresponding PbS molecules, as expected. Our calculated VDE for $(PbS)_2^-$ is 1.70 eV, which is a fair agreement with the experimental value of 1.50 eV. However, there is a slight discrepancy in the computed and measured values of ADE, with the computed ADE being 1.62 eV, while the measured value being 1.30 eV.

*c. $(PbS)_3$/$(PbS)_3^-$.* For the trimer, two isomers were considered for geometry optimization: a bridged trigonal bipyramid and a folded structure which can also be viewed as an edge (PbS) removed cubic structure. Between these two isomers, the trigonal bipyramidal structure with a bridged S atom is found to be the most preferred structure in both the neutral (Fig. 2, 3a) and anionic (Fig. 3, 3a′) clusters. The Pb–S bond lengths in this isomer range from 2.53 Å to 2.77 Å in the neutral trimer, and from 2.58 to 2.65 Å in the anionic case. Interestingly, Pb–Pb interactions continue to be significant in the trimer as they did in the dimer. The Pb–Pb bond length in the S–capped edge of this isomer is 3.25 Å in both the neutral and anion trimer. On the other hand, the folded structure, analogous to two adjacent sides of a cube in which there are no Pb–Pb interactions, is found to be 0.53 eV higher in energy for the neutral trimer (Fig. 2, 3b), while in the case of the anion, it is 0.22 eV higher in energy (Fig. 3, 3b′). The folded (edge-removed cube) structure was reported to be the ground state geometry of neutral $(PbS)_3$ in previously reported theoretical studies. This disagreement between our results and the previously reported results cannot be due to the different functional forms (PW91PW91 in the present case, B3LYP in the previously reported studies), since the energy difference between the edge-capped trigonal bipyramidal structure and the folded structure is quite large in neutral $(PbS)_3$ ($\Delta E = 0.53$ eV) cluster. This disagreement is most likely due to the fact that in the previously reported studies, the authors might not have considered the edge-capped trigonal bipyramidal structure.

Owing to the fact that two isomers in anion are close in energy ($\Delta E = 0.22$ eV), we calculated the ADE and VDE values for both the isomers. The ground state geometry (3a′) yields ADE and VDE values of 2.00 eV and 2.19 eV, respectively. These values are in excellent agreement with the experimental ADE of 1.89 eV and VDE of 2.20 eV. On the other hand, the calculated ADE and VDE values of the higher energy folded structure (3b′) are 2.31 and 2.72 eV, respectively. Since these values are not in agreement with the measured values, we believe that only the edge-capped trigonal bipyramidal structure, and not the folded structure, is present in our cluster beam.

*d. $(PbS)_4$/$(PbS)_4^-$.* The ground state geometry of both neutral and anionic lead sulfide tetramers is a cube with alternating Pb and S atoms. This is the smallest lead sulfide cluster in which there is no Pb–Pb interactions and in which Pb–S bonds govern the stabilization of the cluster. While the neutral $(PbS)_4$ cluster is a perfect cube ($T_d$) with a Pb–S bond length of 2.66 Å (Fig. 2, 4a), its anionic counterpart is a distorted cube (Fig. 3. 4a′), with two distinct Pb–S bond lengths, i.e., 2.65 and 2.74 Å. Our calculated values of the ADE and VDE of $(PbS)_4$ and $(PbS)_4^-$ are 1.47 eV and 1.66 eV, respectively. These values are in good agreement with the corresponding measured values of 1.44 and 1.81 eV.

*e. $(PbS)_5$/$(PbS)_5^-$.* Our calculations revealed two stable and distinct structures for neutral $Pb_5S_5$ cluster: a bi-capped non-planar octagonal structure (Fig. 2, 5a) and a derivative of the cubical structure observed in $(PbS)_4$ with a PbS unit fused to one of the faces of the cube (Fig. 2, 5b), with the 5a isomer being 0.55 eV lower in energy than 5b isomer. In isomer 5b, there is a considerable interaction between two lead atoms with a Pb–Pb bond length of 3.26 Å, while the Pb–S bonds are considerably weakened, with a bond lengths of 2.96 Å. In the $(PbS)_5^-$ anionic cluster, the bi-capped octagonal structure (Fig. 3, 5a′) and the PbS fused lead sulfide tetramer cubic structure (Fig. 3, 5b′) are almost energetically degenerate with an energy difference of 0.06 eV. In order to determine the correct ground state geometry of the $(PbS)_5^-$ anionic cluster, we have calculated the ADE and VDE of both of these isomers. In case of the isomer 5a′, the ADE and VDE are 1.79 eV and 2.00 eV, respectively, while in isomer 5b′, the ADE is calculated to be 2.23 eV and VDE is 3.07 eV. Our measured electron detachment energies from the spectrum are 1.95 eV (ADE) and 2.10 eV (VDE). Upon comparing our calculated ADE and VDE values with that of the experimental values, we conclude that only the bi-capped octagonal structure (isomer 5a′) is present in our cluster beam.

*f. $(PbS)_6$/$(PbS)_6^-$.* Beyond $n = 5$, the geometries of lead sulfide clusters evolve based on the neutral tetramer cube, where either lead sulfide monomer or dimer units are added to the cubic structure. The ground state geometry of the neutral $(PbS)_6$ cluster corresponds to two, face-sharing cubes (Fig. 2, 6a), while a drum structure made up of two hexagonal rings (Fig.2, 6b) is found to be 0.28 eV higher in energy. Even though our ground state geometry is similar to that of the

previously reported studies,[13,14] it does not have a perfect $D_{2h}$ symmetry as reported in these studies. In fact, there are two different Pb–S bond lengths present in this isomer: 2.61 Å and 2.81 Å (see 6a in Fig. 2). The longer bond length is observed when one of the Pb or S atoms are four-fold coordinated, while the shorter bond length corresponds to three-fold coordinated Pb and/or S atoms. In fact, the $D_{2h}$ structure is not found to be a minimum on the neutral potential energy surface.

The presence of an extra electron in the $(PbS)_6^-$ anionic cluster resulted in a distorted face-sharing cubic structure (Fig. 3, 6a′), followed by a higher energy ($\Delta E = 0.27$ eV) cage structure containing four rhombuses, two pentagons, and a hexagon (Fig. 3, 6b′). Interestingly, this higher energy cage structure has one Pb–Pb bond, with a bond length of 3.14 Å. The drum structure (Fig. 3, 6c′) is 0.42 eV higher in energy than the ground state geometry. Compared to the neutral $(PbS)_6$ cluster, the $(PbS)_6^-$ anion has a highly asymmetric structure (Fig. 3, 6a′), with four different Pb–S bonds ranging from 2.60 Å to 2.89 Å in bond length. Since in $(PbS)_6^-$ cluster, there are two isomers (6a′ and 6b′) that are energetically close, we have calculated the electron detachment energies for both of them. The calculated electron detachment energies of the lowest energy structure (6a′) are 1.79 eV (ADE) and 2.00 eV (VDE), which are in excellent agreement with the experimental ADE value of 1.74 eV and VDE of 2.00 eV (see Table II). On the other hand, the VDE and ADE of the cage structure (6b′) are calculated to be 2.38 and 3.14 eV, respectively, and are not in agreement with the corresponding measured values. Thus, we conclude that only the lowest energy isomer (6a′) is making the dominant contribution to the photoelectron spectrum. It should also be noted that the excellent agreement between our calculated and measured ADE values further indicates that the structure of the ground state, neutral $(PbS)_6$ cluster, even though it corresponds to a face-sharing cubes, is not perfectly symmetric as reported in the earlier studies.[14]

*g. $(PbS)_7/(PbS)_7^-$*.   On increasing the number of lead sulfide units to seven, the formation of a symmetric linear array of face-sharing cubes, as was the case in the $(PbS)_6$ neutral, does not occur in neutral $(PbS)_7$. Our calculations show that there are three stable isomers for the $(PbS)_7$ neutral cluster. The lowest energy structure of $(PbS)_7$ corresponds to a highly distorted open-cage structure (Fig. 2, 7a), which can also be described as two distorted cubes fused on the sides. A more symmetric structure (Fig. 2, 7b), in which two cubes share an edge, is found to be 0.10 eV higher in energy. The third structure is a cage containing six rhombuses and two hexagons (Fig. 2, 7c). Our lowest energy structure is not in agreement with the previously reported[14] lowest energy isomer of the neutral $(PbS)_7$ cluster. In the earlier study, the isomer 7c was reported to be the lowest energy isomer. Neither isomer 7a nor isomer 7b was reported in the earlier work.[14]

The ground state structure of the negatively charged $(PbS)_7^-$ cluster is not same as that of its neutral counterpart. In fact, the ground state geometry of the $(PbS)_7^-$ cluster anion is a symmetric structure, in which two cubes are fused along the edge (Fig. 3, 7a′), while a distorted open-cage structure, which is the ground state in neutral $(PbS)_7$, is 0.21 eV higher in energy (Fig. 3, 7b′). The calculated electron detachment energies of the ground state anion (7a′) are 2.12 eV (VDE) and 2.28 eV (ADE), which are in good agreement with the corresponding experimental values of 2.01 eV and 2.22 eV, respectively. On the other hand, the calculated values of ADE and VDE for Isomer 7b′ are 1.86 eV and 2.41 eV, which do not account for the observed peaks in the experiments. Therefore, the structure of the neutral $(PbS)_7$ cluster, obtained as a result of the vertical photodetachment of an electron from $(PbS)_7^-$, corresponds to the isomer containing two edge-shared cubes (7b), rather than the distorted open-cage structure (7a, even though it is the ground state structure of the neutral).

*h. $(PbS)_8/(PbS)_8^-$*.   For the $(PbS)_8$ neutral cluster, two isomers were considered for geometry optimization. The ground state geometry of the $(PbS)_8$ cluster corresponds to a one-dimensional growth of the cubical units (a quadrangular prism), which can be obtained by stacking of three cubes (Fig. 2, 8a). This isomer can also be obtained by adding a $(PbS)_2$ unit to the ground state geometry of $(PbS)_6$ cluster (Fig. 2, 6a) in a linear fashion. On the other hand, if a $(PbS)_2$ unit were to be added on top of $(PbS)_6$, it would result in isomer 8b, which is 0.26 eV higher in energy than the isomer 8a. Isomer 8b can also be obtained by adding a PbS unit to the edge-sharing $(PbS)_7$ cluster (2, 7b). There are three distinct Pb–S bonds present in Isomer 8a, with the Pb–S bond length in the central cube (2.98 Å) being significantly longer than that of the other Pb–S bonds in the cluster. It is also longer than the Pb–S bond length in the $(PbS)_4$ cube (2.66 Å) but very close to the Pb–S bond length in the bulk lead sulfide crystal (2.957 Å).[25] In addition and as expected, the Pb–S bond distances between four-fold coordinated lead and sulfur atoms is larger (2.74 Å) than that of the Pb–S bond distance between three-fold coordinated lead and sulfur atoms (2.62 Å). Based on these bond lengths, the $(PbS)_8$ neutral cluster can be visualized as two weakly interacting $(PbS)_4$ cubes.

The ground state geometry of the $(PbS)_8^-$ cluster anion (Fig. 3, 8a′) is similar to that of its neutral counterpart; however, there is a significant distortion of the central cube due to the extra electron, making this cluster highly asymmetric. The extra electron in the $(PbS)_8^-$ cluster anion has resulted in a further elongation of the Pb–S bond in the central cube to 3.06 Å, thereby weakening the interaction between the two $(PbS)_4$ cubes. The isomer with two-dimensional stacking of cubes (Fig. 3, 8b′) is found to be 0.25 eV higher in energy. The calculated ADE of both of these isomers, 1.89 eV for 8a′ and 1.90 eV for 8b′, are in excellent agreement with the experimentally estimated value of 1.93 eV (See Table II). In addition, the VDE of isomer 8a′ is calculated to be 2.35 eV, while the corresponding value for isomer 8b′ is 2.11 eV, with both being in good agreement with the experimental VDE value of 2.25 eV (Table II). Considering the small energy difference between the isomers (8a′ and 8b′), the nearly identical ADE values, and the similar VDE values, we believe that both the

anionic isomers may be contributing towards the spectrum. However, under the current experimental conditions, we cannot come to a definite conclusion on the existence of multiple isomers.

*i. $(PbS)_9/(PbS)_9^-$.* The addition of a PbS molecular unit to a neutral $(PbS)_8$ cluster results in two isomers of neutral $(PbS)_9$, 9a and 9b (Fig. 2). The ground state geometry of neutral $(PbS)_9$ corresponds to the stacking of four cubes in two dimensions (Fig. 2, 9a) with three distinct Pb–S bond lengths of 2.50, 2.73, and 2.80 Å. The ground state geometry of $(PbS)_9$ can be seen as an extension of isomer, 8b of $(PbS)_8$. A tubular structure with three layers of hexagons (Fig. 2, 9b) is found to be 0.33 eV higher in energy.

The lowest energy geometry of the $(PbS)_9^-$ cluster anion is similar to that of the neutral $(PbS)_9$ cluster (Fig. 3, 9a′). The presence of the extra electron in $(PbS)_9^-$ has again resulted in the elongation of all of the Pb–S bonds as compared to the neutral $Pb_9S_9$. The tubular structure of $(PbS)_9^-$ (Fig. 3, 9b′) is found to be 0.47 eV higher in energy than the lowest energy isomer of $(PbS)_9^-$. Even though the energy difference between the two isomers of $(PbS)_9^-$ is larger than the uncertainty of our theoretical method, we have calculated the electron detachment energies of both of these isomers. Interestingly, the evaluated values of ADE and VDE for both the isomers are close to the observed values from the spectrum. The ADE and VDE values from the photoelectron spectrum are estimated to be 1.99 eV and 2.15 eV, respectively, while the computed ADE and VDE are 1.99 eV and 2.04 eV for isomer 9a′ and 1.85 eV and 2.02 eV for isomer 9b′. Considering the similar computed ADE and VDE values of these isomers and the good agreement with the corresponding experimental values, we cannot eliminate the possibility that both the two-dimensionally stacked cubic structure (Fig. 3, 9a′) and the tubular structure (Fig. 3, 9b′) contribute to the photoelectron spectrum of $(PbS)_9^-$.

*j. $(PbS)_{10}/(PbS)_{10}^-$.* Upon increasing the number of PbS molecular units in the cluster to 10, our calculations show three stable, neutral $(PbS)_{10}$ isomers within the energy difference of 0.21 eV (Fig. 2, 10a, 10b, and 10c). All three isomers correspond to periodic arrays of cubes stacked either in one or two dimensions. The lowest energy isomer of neutral $(PbS)_{10}$ is a symmetric ($C_{2v}$) structure exhibiting two-dimensional stacking of lead sulfide cubical units (Fig. 2, 10a). A quadrangular prism structure (Fig. 2, 10b), obtained by a linear stacking of four cubes, with four distinct Pb–S bonds is found to be 0.13 eV higher in energy than the ground state geometry. Another isomer with two-dimensional stacking of cubes, resulting in an L–shaped structure (Fig. 2, 10c), is found to be 0.21 eV higher in energy.

The lowest energy isomer among $(PbS)_{10}^-$ cluster anions is similar to that of its neutral counterpart with two-dimensional stacking of cubes preferred over the one-dimensional stacking (Fig. 3, 10a′). Interestingly, the quadrangular prism structure (Fig. 3, 10c′) and the L–shaped isomer (Fig. 3, 10b′) were found to be energetically degen-

erate with each other and 0.19 eV higher in energy than isomer 10a′. Following the trend observed in the smaller lead sulfide clusters, the presence of an extra electron in $(PbS)_{10}^-$ cluster has not only resulted in elongation of Pb–S bonds as compared to the corresponding bonds in the neutral cluster, but also resulted in more distorted asymmetric structures. We have calculated the ADE and VDE values for all three isomers and compared them to the values obtained from the $(PbS)_{10}^-$ spectrum. The experimentally determined values for ADE and VDE of $(PbS)_{10}^-$ are 2.08 eV and 2.25 eV, respectively. Interestingly, the computed ADE and VDE values of the three isomers are all in good agreement with the experimental values as listed in Table II. Hence, we can infer that the photoelectron spectrum may be representative of all three anionic $(PbS)_{10}^-$ isomers.

Hence, we infer that the structural evolution of lead sulfide clusters follows a growth pattern of adding cubes in two dimensions. The growth pattern can be generalized as a two-dimensional stacking of cubical units, such that they either share a face or an edge depending upon the number of lead sulfide molecular units in a given cluster.

### 2. $(PbS)_n$ ($n = 11$–15) *clusters*

In Sec. III B 1, we demonstrated that our chosen computational methodology is sufficient to provide good estimates of ADE and VDE values of $(PbS)_n/(PbS)_n^-$ ($n = 1$–10) clusters as well as relative energies among isomers. Encouraged by this success, we have continued our computations on *neutral* lead sulfide clusters up to the nanometer-size regime, i.e., up to $n = 15$. Our aim was to examine the growth pattern of these clusters as a function of the number of PbS molecular units. While small lead sulfide clusters adopt various distorted geometries (in Fig. 2, see structures 3a, 5a, and 7a) as their sizes increase, from $n = 8$ on up in size the lowest energy structures were dominated by cuboidal arrangements of lead sulfide units. Although this is not entirely surprising, we will see that not all cubic arrangements are energetically favorable. As before, for each stoichiometry we have searched several structures. The lowest energy isomers for neutral $(PbS)_n$ ($n = 11$–15) clusters are displayed in Figs. 4 and 5.

The lowest energy structure for neutral $(PbS)_{11}$ can be constructed by adding a PbS unit to $(PbS)_{10}$ (Fig. 2, structure 10a). The addition of a PbS unit will generally be accompanied by the formation of a cube; structures where a PbS unit is left "hanging" (in a low coordination mode) are higher in energy. The Pb-S bond lengths in the structure 11a vary from 2.96 Å to 2.51 Å. As a general rule, for any given neutral lead sulfide cluster, the peripheral Pb-S bonds are shorter and the interior bonds longer. This is due to the high coordination and the increased geometrical strain at the interior of the cluster. Note that longest Pb-S bond length is always in the vicinity of 2.90 to 3.00 Å, which is the average bond length in the bulk lead sulfide.[25]

For $(PbS)_{12}$ neutral clusters, there are two structures within 0.2 eV of one another (Fig. 4, structures 12a and 12b). The lowest energy structure (12a) is obtained by adding a $(PbS)_2$ unit to 10a and the second lowest energy isomer (12b)
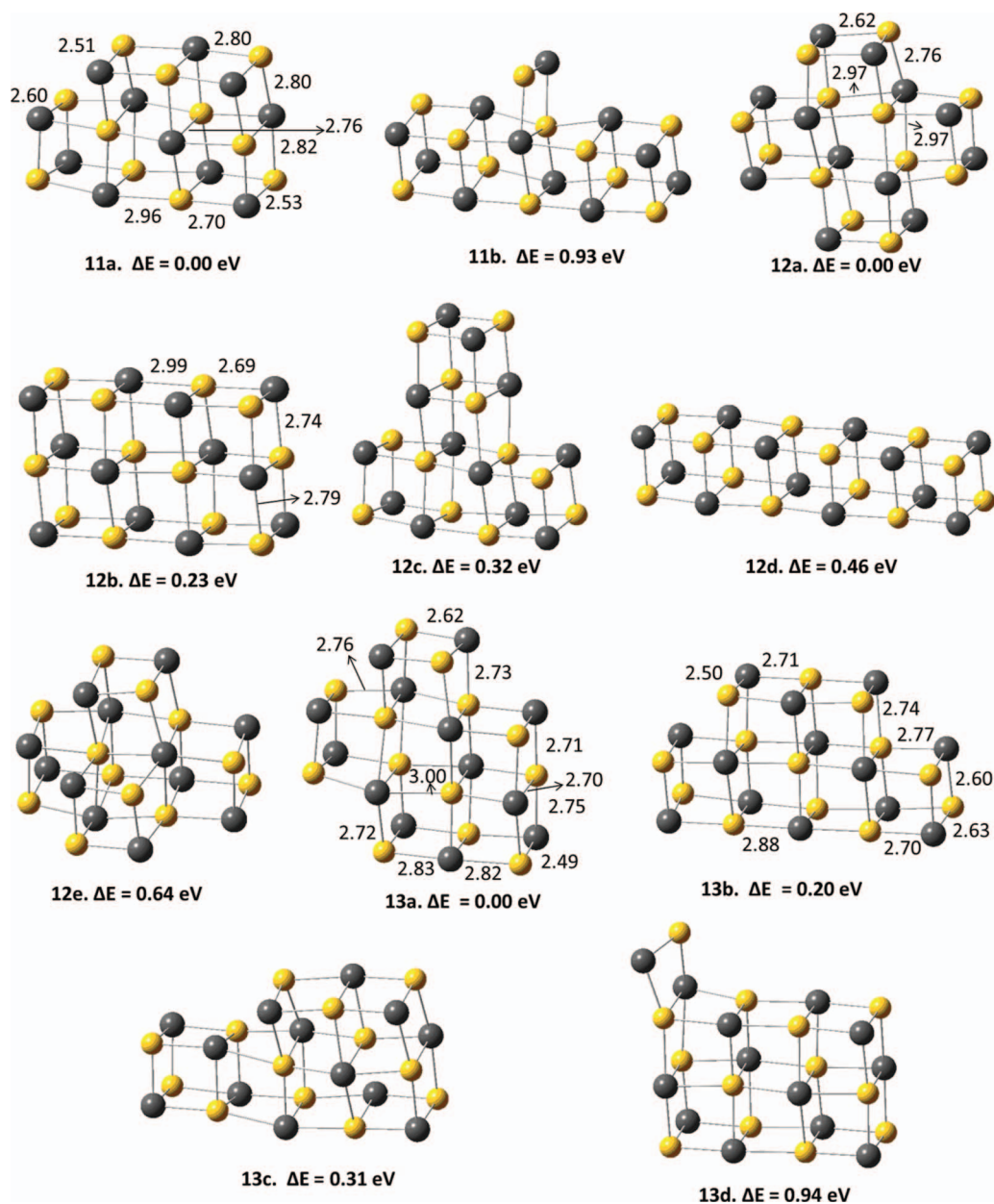
FIG. 4. The lowest energy and higher energy isomers of neutral (PbS)$_n$ ($n = 11$–$13$) clusters. The yellow spheres represent S atoms and the grey ones represent Pb atoms. The bond lengths are given in Å. The relative energy is calculated with respect to the lowest energy structure.

can be formed by adding a PbS molecular unit to 11a. This shows that higher clusters can be constructed either by adding PbS unit to the lower cluster or by adding (PbS)$_2$ unit to the next lower stoichiometric cluster. Fragmentation analysis lends further support to the hypothesis that addition of (PbS)$_2$ units are increasingly preferred.

Similarly, for (PbS)$_{13}$, the two lowest energy isomers (13a and 13b) are derived from 12a and 11a by the addition of a molecular PbS and (PbS)$_2$ units, respectively. Once again, the structures in which PbS units that do not lead to cube formation (13d and 13e) are higher in energy (Fig. 4). The same trend continues for both (PbS)$_{14}$ and (PbS)$_{15}$ clusters as well. Lowest energy isomers of all these clusters can be directly traced back to their smaller clusters.

In addition to these structures, there are two other cluster types worth mentioning. First, there is the quadrangular

prism (QP): which is a linear (one-dimensional) arrangement of cubes. As the size of the cluster increases, the preference for quadrangular prism steadily decreases. For example, for $n = 10$, 12, and 14 cluster sizes, the relative energy differences between the most stable structures and the QP structures are 0.13 eV, 0.46 eV, and 0.54 eV, respectively. This is understandable because as the sizes of the clusters increase, the preference for "clusterization," where more and more atoms attain higher coordination, also increases. The lowest energy isomers considered here have one thing in common; the maximum coordination number that all the lead and sulfur atoms adopt is five. In other words, all the isomers are either one- or two-dimensional stacking of cubes. What about clusters where at least some atoms are six-fold coordinated? Note that in the bulk all lead and sulfur atoms have hexacoordination. In order to understand the energy preference for
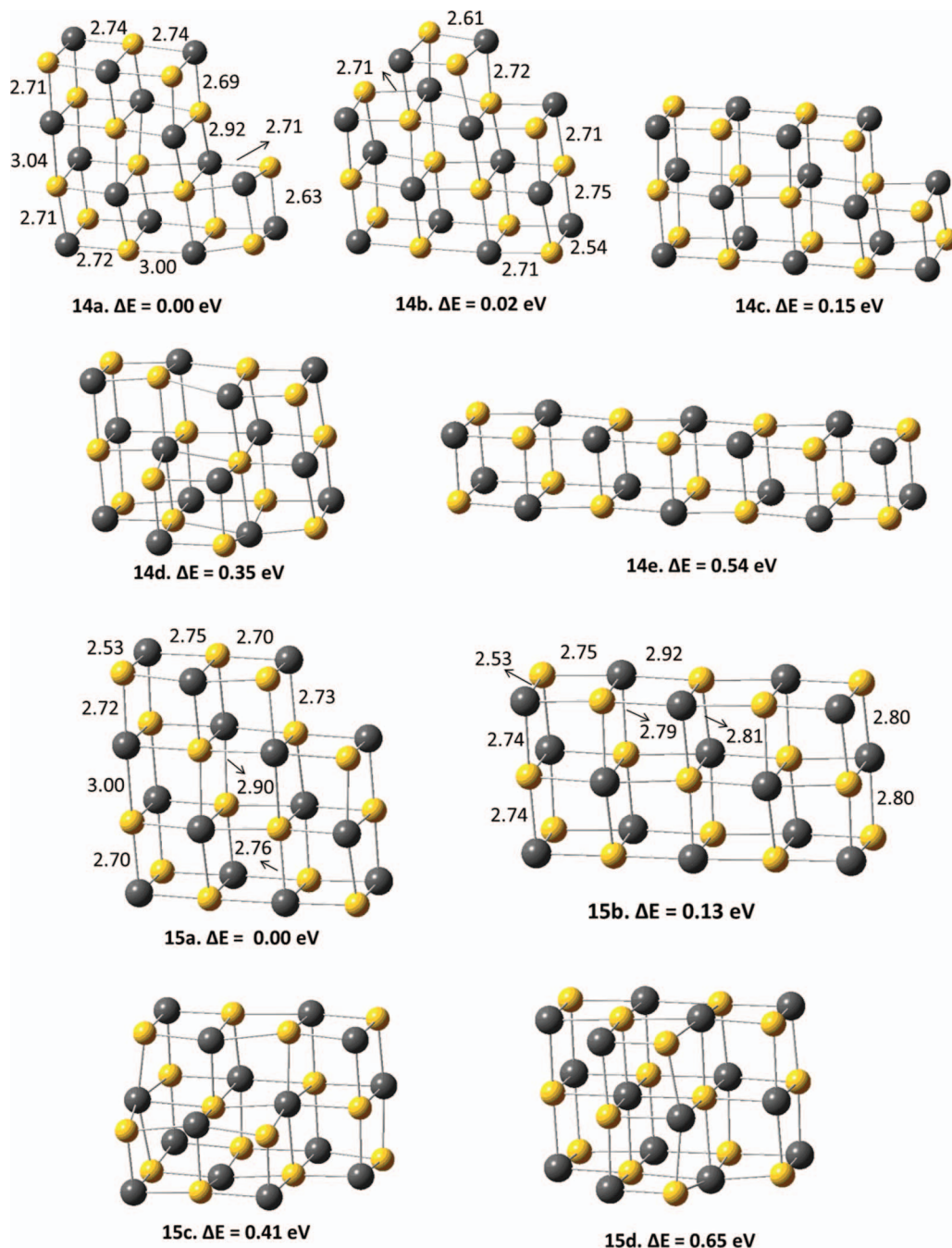
FIG. 5.  The lowest energy and low-lying isomers of neutral (PbS)$_n$ ($n$ = 14–15) clusters. The yellow spheres represent S atoms and the grey ones represent Pb atoms. The bond lengths are given in Å. The relative energy is calculated with respect to the lowest energy structure.

bulk-like clusters, we have studied isomers where at least one PbS unit is hexa-coordinated, as in 12e, 14d, 15c, and 15d. In all these isomers, the coordination around central PbS unit is similar to that of the bulk structure. Our calculations indicate that these isomers are 0.64 eV, 0.35 eV, 0.41 eV, and 0.65 eV, respectively, higher in energy than the corresponding lowest energy structures. Although, the cluster size has reached nanometer scale (the diameter in (PbS)$_{15}$ is 12 Å), the geometrical strain, as reflected in Pb-S bond lengths, associated in the formation of hexa-coordination is not sufficiently compensated for the cluster sizes considered in the current study.

### 3. Stability and energetics of (PbS)$_n$ ($n$ = 1–15) clusters

The calculated HOMO–LUMO (HL) gaps of (PbS)$_n$ ($n$ = 1–15) neutral clusters are plotted in Fig. 6. For the most part, the HOMO–LUMO gaps of lead sulfide clusters oscillate with size, although their values also tend to decrease with increasing size, e.g., (H-L) gaps = 2.95 eV in (PbS)$_2$ but 1.92 eV in (PbS)$_{13}$. Significantly, the (PbS)$_4$ cluster has the largest H-L gap, at 2.96 eV.

Interestingly, in an experimental study a few years ago,[8] it was reported that sub-nanometer-size, uncapped lead sulfide QDs, synthesized via electroporation of synthetic
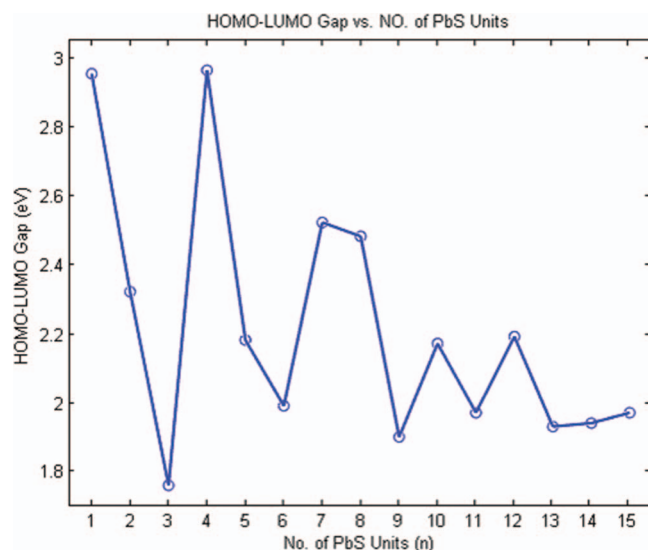
FIG. 6. HOMO–LUMO gap (in eV) of neutral $(PbS)_n$ ($n = 1$–$15$) clusters as a function of $n$, the number of PbS units.
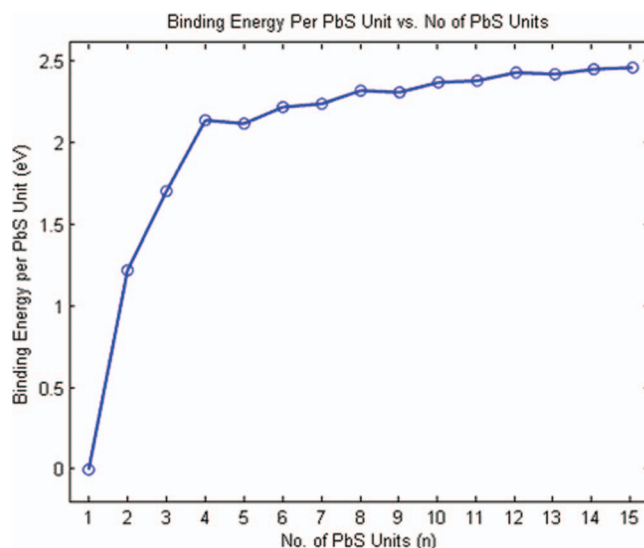


FIG. 7. $E_b$, the binding energy per PbS unit of neutral $(PbS)_n$ ($n = 1$–$15$) clusters (from Eq. (1)) as a function of $n$, the number of PbS units.

vesicles, exhibited time-dependent, oscillating red and blueshifts of their UV absorption bands. These QDs were characterized as being smaller than 1 nm (3–10 Å) and reportedly corresponded to $(PbS)_n$ ($n = 1$–$9$) clusters. In addition, beyond the size corresponding to $n = 8$, a monotonic redshift of the absorption band was observed. Our calculated results exhibit an oscillating trend in the H-L gaps up to $n = 13$, with a sharp drop in H-L gap values beginning at $n \sim 9$, and a minimal change in the H-L gap beyond $n = 13$. Curiously, our theoretical results appear to track the above-mentioned experimental results.[8]

The binding energy per PbS unit, $E_b$, of neutral $(PbS)_n$ ($n = 1$–$15$) clusters is calculated from the following equation:

$$E_b = \frac{-[E(PbS)_n - nE(PbS)]}{n}. \tag{1}$$

These $E_b$ values as a function of the number of PbS units ($n$) are plotted in Fig. 7. The $E_b$ values increased dramatically with the number of PbS units between $n = 2$–$4$. Beyond $n = 4$, the change in binding energy per PbS unit is minimal, with even $n$ clusters exhibiting slightly larger binding energies than odd $n$ clusters. The nearly saturated binding energies beyond $n = 4$ may be due to structural similarities among larger $(PbS)_n$ clusters, possibly due to the presence of cubical $(PbS)_4$ motifs.

In order to study the thermodynamic stability of $(PbS)_n$ clusters, we have calculated the fragmentation/dissociation energies along different pathways using the following equations:

Fragmentation losing PbS

$$= -[E(PbS)_n - E(PbS)_{n-1} - E(PbS)], \tag{2}$$

Fragmentation losing $(PbS)_2$

$$= -[E(PbS)_n - E(PbS)_{n-2} - E(PbS)_2], \tag{3}$$

Fragmentation losing $(PbS)_4$

$$= -[E(PbS)_n - E(PbS)_{n-4} - E(PbS)_4]. \tag{4}$$

The fragmentation energies are calculated by considering the ground state energies of both the parent and the product clusters. The fragmentation energies calculated here provide us with a gauge of the stabilities of these clusters.

In Fig. 8, we show fragmentation energies as a function of $n$ for the above three product outcomes. From Fig. 8, it is evident that $(PbS)_4$ exhibits unusually high stability compared to its neighboring clusters. (It is more difficult to fragment.) In addition, the fragmentation/dissociation resulting in $(PbS)_4$ as a product cluster is found to be consistently the most preferred fragmentation pathway for all of the $(PbS)_n$ clusters in the present study. Among all the clusters, $(PbS)_8$ requires the least amount of energy (1.39 eV) to dissociate it into two $(PbS)_4$ clusters. This scenario is consistent with the structure of $(PbS)_8$ discussed earlier, where the ground state geometry of $(PbS)_8$ can be seen as two weakly interacting $(PbS)_4$ cubic units. The fragmentation pathway leading to PbS and



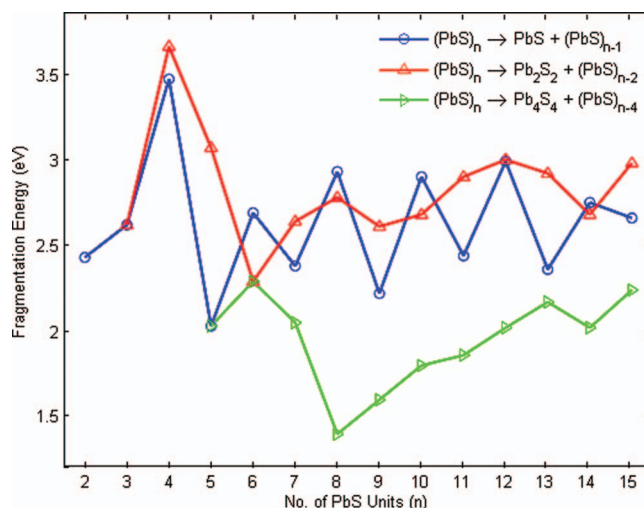FIG. 8. Fragmentation energies of neutral $(PbS)_n$ ($n = 1$–$15$) clusters into different fragmentation paths (from Eqs. (2)–(4)) as a function of $n$, the number of PbS units.

$(PbS)_{n-1}$ units exhibits an odd–even alteration, with clusters comprising even numbers of PbS units being more stable than clusters with odd values of $n$, indicating that the PbS units prefer to add in pairs, i.e., $(PbS)_2$. This is also consistent with the odd–even alteration observed in the electron detachment energy values, where the clusters with even $n$ have a lower ADE than the clusters with odd $n$.

It is well known in gas-phase cluster physics that during the fragmentation of larger clusters, the most preferred fragmentation pathway often leads to the most stable species, i.e., a magic number cluster. A magic cluster is typically characterized by unusually high stability compared to its immediate neighbors, a large H-L gap, and a smaller EA value than that of its immediate neighbors. The $(PbS)_4$ cluster satisfies all these criteria and can, thus, be classified as a magic cluster.

## IV. CONCLUSIONS

In summary, negatively charged $(PbS)_n^-$ ($n = 1–10$) clusters were generated in the gas-phase and characterized using anion photoelectron spectroscopy. The observed electron detachment energies of these clusters show an odd-even alteration up to $n = 8$. Among the clusters considered in this study, $(PbS)_4^-$ has the lowest ADE of 1.47 eV. For small clusters ($1 < n < 5$), our calculations found that the structures with Pb–Pb bonds were either ground state geometries or energetically competitive. Beyond $n = 5$, isomers containing Pb–S bonds were found to be preferred. Furthermore, the energetics (fragmentation, H-L gaps) pertaining to the structural evolution of these clusters indicate that the $(PbS)_4$ is a magic cluster.

Furthermore, in neutral $(PbS)_n$ ($n = 11–15$) nanoclusters, there is a strong preference for forming structures based on the two-dimensional stacking of cubes, in which the Pb and S atoms prefer a maximum of five-fold coordination. This observation raised an important question: At what cluster size of $(PbS)_n$ does the transition to bulk-like structures occur, i.e., where the Pb and S atoms have a six-fold coordination. Thus, one might expect a change in the optical properties of $(PbS)_n$ clusters when they undergo a structural transition from a two-dimensional layered structure to a bulk-like structure. A systematic study focusing on the structural evolution of $(PbS)_n$ nanoclusters with size is vital for understanding their size-dependent optical properties. A computational investigation in this direction is currently underway.

[1] J. L. Machol, F. W. Wise, R. C. Patel, and D. B. Tanner, Phys. Rev. B **48**, 2819 (1993).
[2] E. A. Albanesi, E. L. Peltzer y Blanca, and A. G. Petukhov, Comput. Mater. Sci. **32**, 85 (2005).
[3] Y. Saito, K. Mihama, and T. Noda, Jpn. J. Appl. Phys. **22**, L179 (1983).
[4] Y. Saito, M. Suzuki, T. Noda, and K. Mihama, Jpn. J. Appl. Phys. **25**, L627 (1985).
[5] R. A. Teichman and E. R. Nixon, J. Mol. Spectrosc. **54**, 78 (1975); C. P. Marino, J. D. Guerin, and E. R. Nixon, *ibid*. **51**, 160 (1974).
[6] R. Colin and J. Drowart, J. Chem. Phys. **37**, 1120 (1962).
[7] C. A. Fancher, H. L. de Clercq, and K. H. Bowen, Chem. Phys. Lett. **366**, 197 (2002).
[8] S. Wu, H. Zeng, and Z. A. Schelly, Langmuir **21**, 686 (2005).
[9] L. Cademartiri, E. Montanari, G. Calestani, A. Migliori, A. Guagliardi, and G. A. Ozin, J. Am. Chem. Soc. **128**, 10337 (2006).
[10] P. E. Lippens and M. Lannoo, Phys. Rev. B **39**, 10935 (1989).
[11] R. S. Kane, R. E. Cohen, and R. Silbey, J. Phys. Chem. **100**, 7928 (1996).
[12] G. E. Tudury, M. V. Marquezini, L. G. Ferrir, L. C. Barbosa, and C. L. Cesar, Phys. Rev. B **62**, 7357 (2000).
[13] H. Zeng, Z. A. Schelly, K. Ueno-Noto, and D. S. Marynick, J. Phys. Chem A. **109**, 1616 (2005).
[14] J. He, C. Liu, F. Li, R. Sa, and K. Wu, Chem. Phys. Lett. **457**, 163 (2008).
[15] K. M. McHugh, H. W. Sarkas, J. G. Eaton, C. R. Westgate, and K. H. Bowen, Z. Phys. D: At., Mol. Clusters **12**, 3 (1989).
[16] J. V. Coe, J. T. Snodgrass, C. B. Freidhoff, K. M. McHugh, and K. H. Bowen, J. Chem. Phys. **84**, 618 (1986).
[17] M. J. Frisch, G. W. Trucks, H. B. Schlegel *et al.*, GAUSSIAN 03, Revision C.02, Gaussian, Inc., Wallingford, CT, 2004.
[18] J. P. Perdew and Y. Wang, Phys. Rev. B **45**, 13244 (1992); J. P. Perdew, K. Burke, and Y. Wang, *ibid*. **54**, 16533 (1996).
[19] W. J. Stevens, M. Krauss, H. Basch, and P. G. Jasien, Can. J. Chem. **70**, 612 (1992).
[20] A. D. Becke, J. Chem. Phys. **98**, 5648 (1993).
[21] C. Lee, W. Yang, and R. G. Parr, Phys. Rev. B **37**, 785 (1988).
[22] W. Kuechle, M. Dolg, H. Stoll, and H. Preuss, Mol. Phys. **74**, 1245 (1991).
[23] T. M. Miller and W. C. Lineberger, Int. J. Mass Spectrom. Ion Process. **102**, 239 (1990).
[24] C. Jin, K. J. Taylor, J. Conceica, and R. E. Smalley, Chem. Phys. Lett. **175**, 17 (1990).
[25] Y. Noda, K. Masumoto, S. Ohba, Y. Saito, K. Toriumi, Y. Iwata, and I. Shibuya, Acta Crystallogr., Sect. C: Cryst. Struct. Commun. **43**, 1443 (1987).